Evaluation of a SQUID-based receiver for transient electromagnetics in Bad Frankenhausen, Germany

Raphael Rochlitz[1], Thomas Günther[1], Matthias Queitsch[2], Nina Kukowski[2], Andreas Chwala[3], and Ronny Stolz[3]

[1]*Leibniz Institute for Applied Geophysics - Hannover, Germany*
[2]*Friedrich Schiller University - Jena, Germany*
[3]*Leibniz Institute of Photonic Technology - Jena, Germany*

Abstract

Within the framework of the multidisciplinary research project called INFLUINS, INtegrated FLUid dynamics IN Sedimentary basins, we use a highly sensitive magnetic field receiver based on Superconducting Quantum Interference Devices (SQUIDs) for the transient electromagnetic method and compare its performance specifications with a commercially available induction coil.
Four fixed loops TEM measurements with 10 - 20 receiver stations each have been conducted along a survey line perpendicular to the known geologic strike direction at the test site *Esperstedter Ried* in Northern Thuringia, Germany.
The signals of the SQUID receiver provide significantly better quality and are less affected by natural and man-made noise sources than the ones of the induction coil, which is proved by data error and noise measurement analysis. As a result, the 1D inverse modeling results of the SQUID data show lower misfit ratios and are more reliable compared to the coil.

1 Introduction

In transient electromagnetic (TEM) surveys, usually the time derivative dB_z/dt of the vertical magnetic field component B_z is recorded with induction coil receivers. Alternatively, it is possible to measure directly the vector components B_x, B_y and B_z with magnetic field sensors, so-called magnetometers, which shows several advantages pointed out by Asten & Duncan, (2012).
Until 1990, only induction coil receivers were used for TEM due to the fact that magnetic field sensors did not provide the desired accuracy to compete with them (Telford, 1990). Especially since the beginning of the 21st century, the development of highly accurate B-field receivers based on Superconducting QUantum Interference Devices (SQUIDs) lead to new opportunities for TEM measurements.
Today, especially low- and high-temperature supcerconductor SQUIDs, named LTS and HTS, are in routine field use as receivers for TEM exploration surveys (Le Roux & Macnae, 2007; Chwala et al., 2011; Vallée et al., 2011; Smith, 2014). In all these studies, LTS SQUID sensors clearly outperform other magnetic field receivers such as HTS SQUIDs, optically pumped magnetometers (OPM) and fluxgate magnetometers as well as conventional or specially developed induction coils.

Successful exploration studies in low-noise areas are described by Le Roux & Macnae, (2007), Webb & Corscadden, (2009) and Smit & Le Roux, (2009). In this work, we applied an LTS SQUID based magnetometer for TEM in a culturally disturbed environment, the test site *Esperstedter Ried*, and evaluate the performance specifications of this SQUID receiver in comparison with a commercially available induction coil.
Subsequently, the survey area and the field measurements are introduced. Afterwards, decay curves, data errors, noise records and first inverse modeling results are presented. It is concluded with a summary of important results and an outlook towards future work.

2 Survey details

2.1 Investigation area

The survey area, which includes the Esperstedter Ried, is situated in the East of Bad Frankenhausen (Fig. 1) in northern Thuringia, Germany. This area is of great interest for geological surveys due to subrosion effects, observed since decades (PGL, 1926). For our TEM survey, especially two facts are important. On the one hand, saline waters, which even reach the surface, lead to a highly conductive overburden, and thus, to theoretical advantages for the *B*-field receiver (Asten & Duncan, 2012). On the other hand, data of an additional seismic and large-scale ERT survey, described by Rochlitz, (2015), are available at the test site, which enables to better interpret the recorded TEM data.

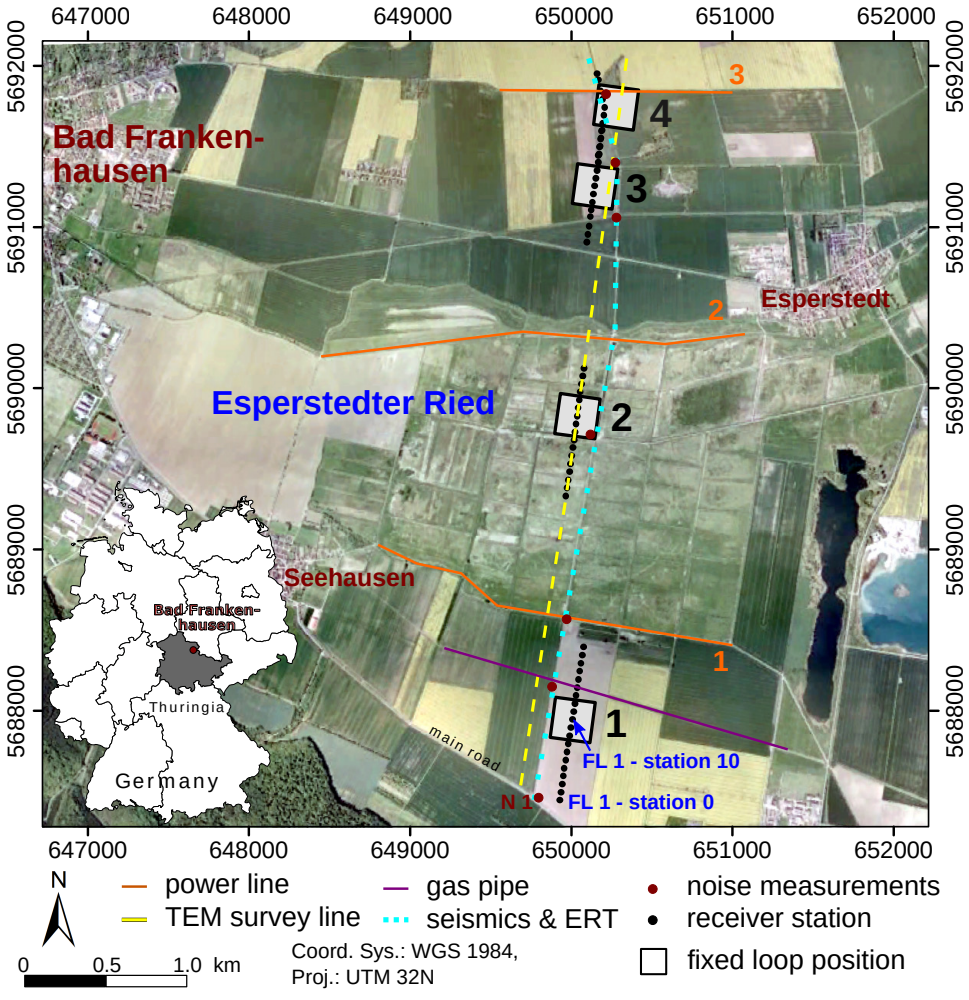

Figure 1: Test site *Esperstedter Ried* near Bad Frankenhausen and survey design.

2.2 Instruments

The transmitter equipment, depicted in Fig. 2 a), consists of the following instruments:

- 9 x 12 V batteries
- Crone - PEM transmitter - max. current: 20 A
- EMIT - SMARTem transmitter controller - waveform adjustment and timing

The receiver systems, shown in Fig. 2 b), are described below:

- 3-component LTS SQUID receiver
- Supracon - SQUID sensor controller, called OrangeBox
- 1-component (B_z) Crone receiver coil
- EMIT SMARTem24 field computer - 12 channels with 24 bit ADCs

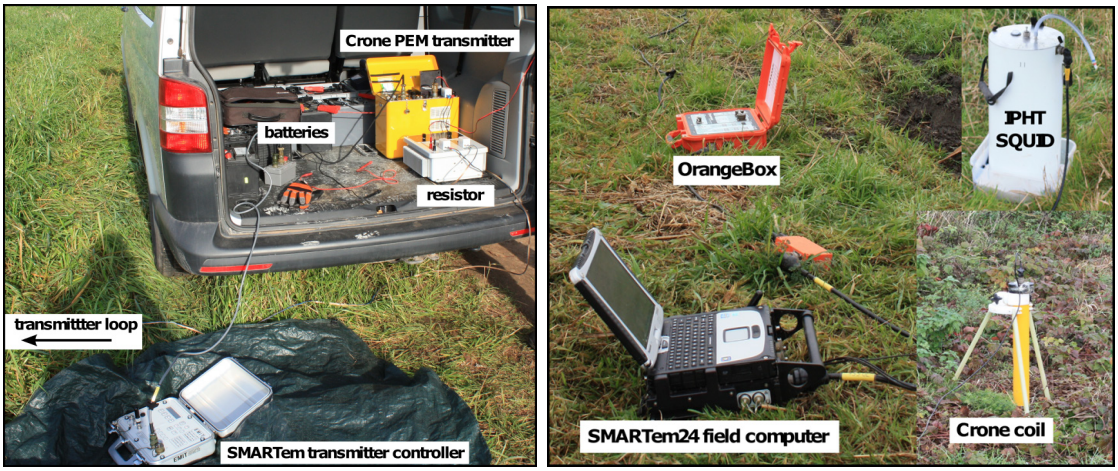

(a) Transmitter unit **(b)** Receiver unit

Figure 2: TEM instruments.

2.3 Survey information

The survey took place from 17th - 21st November 2014. In order to reach an optimum signal to noise ratio (SNR) with a maximum amount of measured data, we decided for the fixed loop configuration, which provides a comparatively high source signal strength with low logistic effort, since the transmitter loop (Tx) needs to be placed only once to cover 1 km of the survey line. Four fixed loops with 10 - 20 receiver stations each were placed along a survey line (Fig. 1) with gaps due to power lines and gas pipes. Furthermore, noise measurements were conducted in order to characterize the two different receiver systems and the electromagnetic noise at different locations within the test site. Important survey parameters are listed below:

- Transmitter current: 11.8 - 11.0 A (decreasing with battery voltage)
- Transmitter loop size: 250 x 250 m, receiver station offset: 50 m
- 50 % duty cycle: 2 s / 0.5 Hz, downward ramp: 85 μs
- Number of gates: 39
- Number of stacks within one reading: 128
- Number of readings: 5 - 11 depending on noise level

3 Results

3.1 Noise measurements

In Figs. 3 a) and b), the noise record N 1 (Fig. 1) at FL 1 adjacent to the main road, is presented in time and frequency domain, respectively. As expected, only the horizontal components of the SQUID as well as the coil are affected by sferics (Fig. 3 a). The SQUID-Z signal is approximately constant over time, whereas the coil signal varies, which can be attributed to the traffic and the higher spatial sensitivity of the coil. Especially at frequencies less than 100 Hz and explicitly at 50 Hz, the SQUID-Z noise is significantly lower, as can be observed in Fig. 3 b).

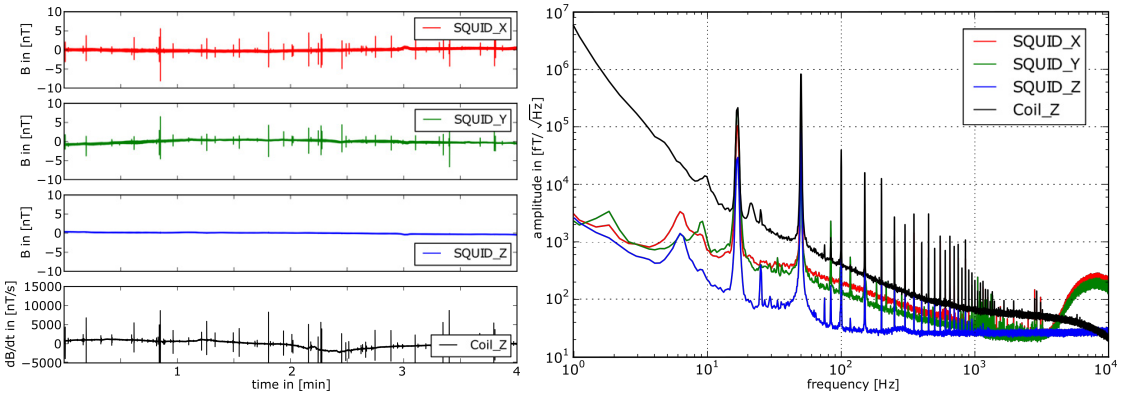

(a) **(b)**

Figure 3: Noise measurements in 50 m distance to the main road: a) time-domain, b) frequency-domain.

3.2 SQUID and coil decays

As an example, decay curves of both receivers are depicted at two locations: the central loop position of FL 1 (Fig. 4 a) and the receiver station adjacent to the main road (Fig. 4 b). The Z-component of the SQUID sensor shows a significantly better data quality compared to the coil at times later than 100 ms at both positions. The horizontal components are added for the sake of completeness, but are not discussed for brevity.

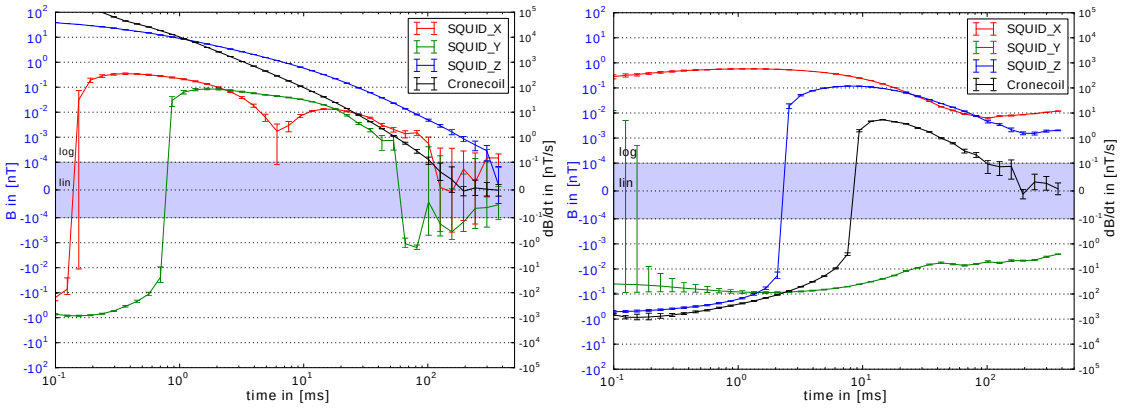

(a) FL 1 - station 10, central loop pos. (Fig. 1) **(b)** FL 1 - station 0, adjacent to main road (Fig. 1)

Figure 4: Decay curve examples.

3.3 Data errors

In order to deliver a quantitative representation of data errors, the normalized standard deviation was calculated for every time gate at all receiver stations. In Fig. 5, the percentage data error is illustrated for the Z-components of all receiver stations at FL 1. Overall, the SQUID sensor shows better data quality after 100 ms (red line in Fig. 5). Furthermore, it is less affected by the gas pipe and the power line, but shows higher data errors at early times < 10 ms close to the road. The noisy gates around the polarity switch at out-of-loop receiver positions occur earlier in the B-field signal. Thus, there is an advantage at late times, especially at offsets greater than 300 m to the center of Tx.

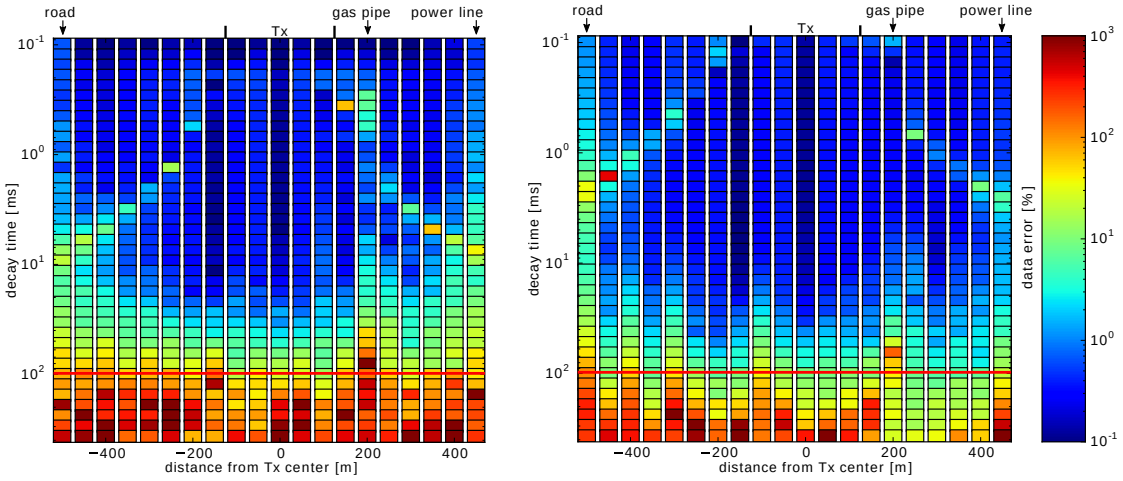

(a) Coil **(b)** SQUID-Z

Figure 5: Data errors (normalized standard deviation) for each time gate and every receiver station of FL 1, red line = 100 *ms* decay time.

3.4 Inverse modeling results

In general 1D Levenberg-Marquardt inverse modeling results by using the code *Beowulf* (Raiche, 2008) do not significantly vary in terms of layer depths and resistivities between coil and SQUID-Z data. An example, the 1D inverse modeling results of the FL 1 dataset, based on the same starting model, is presented in Fig. 6. The 1D starting model with 7 layers is based on a trial-and-error fit at the central loop position of Fl 1. For more information, it is referred to Rochlitz, (2015).

The coil data inversion (Fig. 6 a) shows more artifacts, which occur at the road, the gas pipe and the power line, whereas inverse modeling results of the SQUID-Z component (Fig. 6 b) are solely disturbed by the gas pipe. Furthermore, in the central part, the obtained resistivity distribution from the SQUID-Z data appears more consistent in respect to an approximately 1D subsurface structure in the uppermost 300 m (Rochlitz, 2015).

In order to gain a first quantitative view of the inversion quality, it is possible to calculate the misfit ratio between the measured data and the final forward response for each time gate and receiver station. The misfit ratios according to the previously presented *Beowulf* 1D inverse modeling results of Fl 1 are depicted in Fig. 7. Considering the logarithmic color scale, the overall misfit ratio of the SQUID data inversion (Fig. 7 b) is significantly lower than the one of coil data inversion (Fig. 7 a).

Another important fact is that the misfit ratio related to the SQUID shows nearly a Gaussian distribution. Exceptions occur only due to the gas pipe and polarity switches. In contrast, particularly at early times until 1 ms, the misfit ratio related to the coil is systematically biased according to in-loop and out-of-loop receiver stations. Surprisingly, this fact has no noticable impact on the inverse modeling results, depicted in Fig. 6.

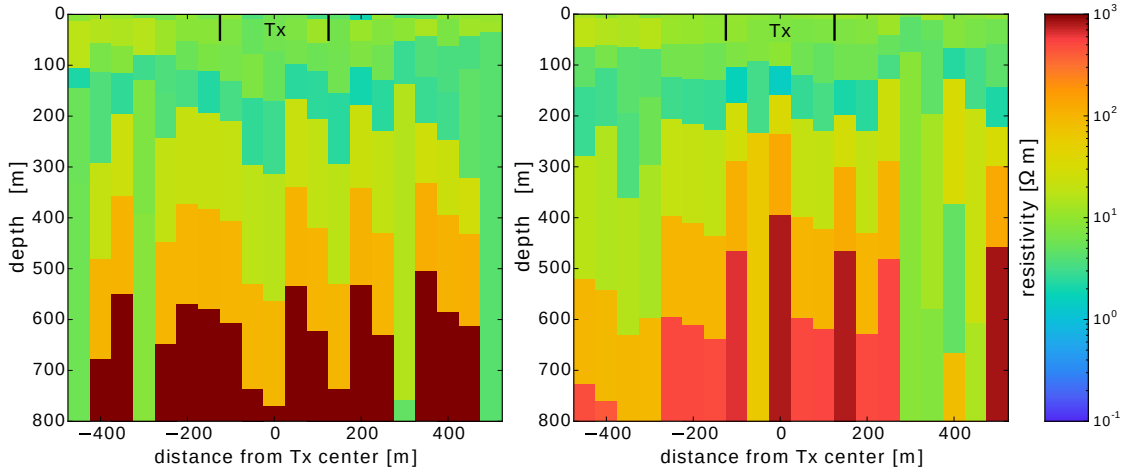

(a) Coil **(b)** SQUID-Z

Figure 6: Coil and SQUID-Z 1D inversion results of the FL 1 dataset

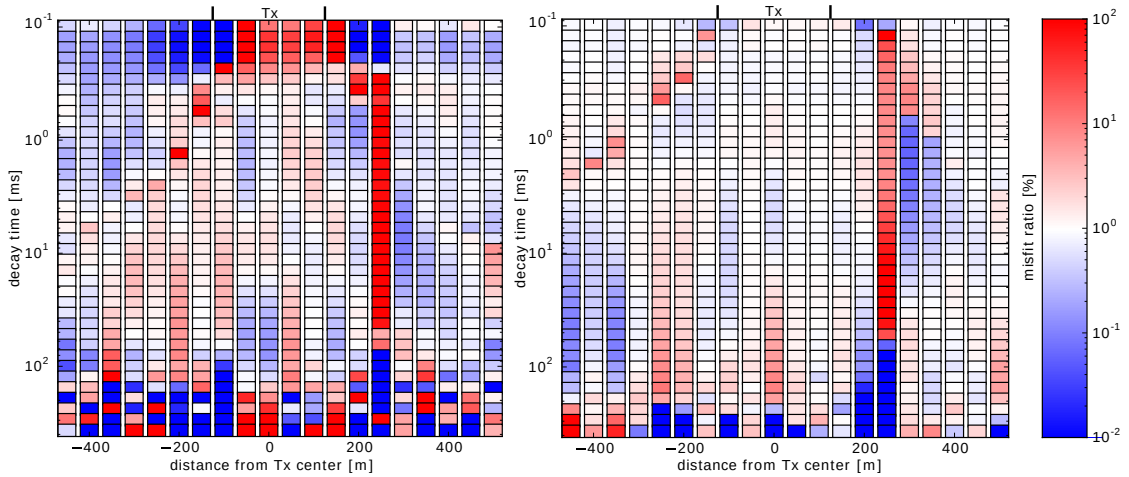

(a) Coil **(b)** SQUID-Z

Figure 7: Coil and SQUID-Z inversion misfit ratio according to the results in Fig. 6.

4 Summary and Outlook

We applied an LTS SQUID-based magnetic field receiver in comparison with a commercially available induction coil for TEM measurements. It was focused on the presentation of the results according to the datasets of FL 1. Nevertheless, the obtained results, summarized subsequently, are valid for the data of the other 3 fixed loop positions within our test site as well (Rochlitz, 2015).

The SQUID sensor shows advantages over the coil in every respect: The average usable decay time range of the SQUID is significantly larger, as can be inferred from decay and data error figures. The better data quality can be first explained by theoretical advantages, especially the slower decaying B-field (Asten & Duncan, 2012). Second, in particular the SQUID-Z component is less affected by sferics, traffic and power lines than the coil, as noise measurements indicate. Furthermore, 1D *Beowulf* inversion results of the SQUID have advantages over the coil with respect to misfit ratios and reliability of the 1D approach.

A more detailed description of the inverse modeling procedure and the geological interpretation of the final inversion results along the survey line in accordance with the seismic and ERT data (section 2.1) can be obtained in Rochlitz, (2015).
Inverse modeling of SQUID and coil data with alternative software is still in progress. Most important, in order to gain maximum advantage of using the LTS SQUID, the 3-component data should be inverted altogether. It is assumed that the uncertainty, which results from the principle of equivalence, will be reduced. Furthermore, it would be advantageous to consider data errors and apply a laterally constrained 1D inverse modeling procedure.

Acknowledgements

The Leibniz Institute of Photonic Technology and the Supracon AG as well as the Friedrich Schiller University Jena provided not only the instruments for this TEM study, but also supported conducting the survey. Special thanks goes to Frank Bauer and Stefan Dunkel. The survey was funded by the Federal Ministry of Education and Research (BMBF) as part of INFLUINS (grant 03IS2091A).

References

Asten, M. W., & Duncan, A. C. (2012). The quantitative advantages of using B-field sensors in time-domain EM measurement for mineral exploration and unexploded ordnance search. *Geophysics*, *77*(4), WB137–WB148.

Chwala, A., Smit, J., Stolz, R., Zakosarenko, V., Schmelz, M., Fritzsch, L., et al. (2011). Low temperature SQUID magnetometer systems for geophysical exploration with transient electromagnetics. *Superconductor Science and Technology*, *24*(12), 125006 ff.

Le Roux, C., & Macnae, J. (2007). SQUID sensors for EM systems. In *Exploration in the new millennium: Proceedings of the fifth decennial international conference on mineral exploration* (pp. 417–423).

PGL - Preußische Geologische Landesanstalt. (1926). *Erläuterungen zur Geologischen Karte von Preußen und benachbarten deutschen Ländern.* Berlin.

Raiche, A. (2008). The P223 software suite for planning and interpreting EM surveys, PREVIEW. *Australian Society of Exploration Geophysicists*, *Issue 132*, 25-30.

Rochlitz, R. (2015). *Squid-based transient electromagnetics in an area with highly conductive overburden - a case study from Bad Frankenhausen, Thuringia.* Master's thesis, FSU Jena, Germany.

Smit, J., & Le Roux, T. (2009). TDEM survey at Shea Creek uranium deposit utilising a low-temperature superconductor SQUID. In *11th SAGA biennial technical meeting and exhibition.*

Smith, R. (2014). Electromagnetic induction methods in mining geophysics from 2008 to 2012. *Surveys in Geophysics*, *35*(1), 123–156.

Telford, W. M. (1990). *Applied geophysics.* Cambridge England New York: Cambridge University Press.

Vallée, M. A., Smith, R. S., & Keating, P. (2011). Metalliferous mining geophysics—state of the art after a decade in the new millennium. *Geophysics*, *76*(4), W31–W50.

Webb, M., & Corscadden, B. (2009). A case study of deep electromagnetic exploration in conductive cover. *ASEG Extended Abstracts*, *2009*(1), 1–11.